Resonance Pacemakers in Excitable Media

Tabitha Ruvarashe Chigwada,[1] P. Parmananda,[2,3] and Kenneth Showalter[1]

[1]*Department of Chemistry, West Virginia University, Morgantown, West Virginia 26506-6045, USA*
[2]*Facultad de Ciencias, UAEM, Avenida, Universidad 1001, Colonia Chamilpa, Cuernavaca, Morelos, Mexico*
[3]*Centro de Ciencias Físicas, UNAM, Cuernavaca 62210, Morelos, Mexico*

(Received 13 February 2006; published 19 June 2006)

Chemical waves are initiated in an excitable medium by resonance with local periodic forcing of the excitability. Experiments are carried out with a photosensitive Belousov-Zhabotinsky medium, in which the excitability is varied according to the intensity of the imposed illumination. Complex resonance patterns are exhibited as a function of the amplitude and frequency of the forcing. Local resonance-induced wave initiation transforms the medium globally from a quiescent excitable steady state to a periodic state of successive traveling waves.

DOI: 10.1103/PhysRevLett.96.244101 PACS numbers: 82.40.Bj, 05.45.−a, 05.65.+b, 47.54.−r

The most common source of wave initiation in excitable media is a localized oscillatory region that serves as a pacemaker, emitting successive waves into the medium. In the Belousov-Zhabotinsky (BZ) reaction [1], dust particles or other heterogeneities cause the system to become locally oscillatory, and waves emanate from these sources at the frequency of the local oscillation [2–6]. Waves can also be initiated with a desired frequency at a silver electrode by electrochemically removing the bromide ion [7,8], an inhibitor of autocatalysis in the BZ reaction [9]. It is likely that the surface adsorption of bromide (or bromine) is responsible for the spontaneous pacemakers at heterogeneities such as dust particles. Self-sustaining spiral waves are another common wave source; however, spirals do not spontaneously appear in quiescent excitable media. Spiral waves may be deliberately generated by breaking a wave, for example, by mechanical agitation of a BZ solution or by erasing part of a circular wave [1,3,10–12]. Spiral waves occur spontaneously in heterogeneous media, such as heart tissue [11,13–15] or heterogeneous BZ media [16–18]. Specific initial conditions also give rise to spiral waves, the most common being cross field stimulation [13,19] and wave initiation in the wave back or ''vulnerable region'' of a propagating wave [20,21].

In this Letter, we present a new type of wave source in excitable media, a resonance-induced pacemaker. Resonance wave initiation is not dependent on the system parameters crossing into the oscillatory regime, as with oscillatory pacemakers, but relies on small amplitude modulations of the local excitability [22]. Sustained wave initiation is exhibited with an appropriately tuned amplitude and frequency, which may occur in complex patterns with respect to the driving frequency. In all cases, wave initiation occurs without varying the system parameters into the oscillatory regime.

Experiments were carried out using a photosensitive BZ gel medium, with the ruthenium(II)-bipyridyl complex as the light-sensitive catalyst [23,24]. This catalyst is excited by 460 nm light, and its excited state reacts with the bromomalonic acid reactant to produce bromide ions [25]. The excitability of the system can therefore be adjusted by varying the light intensity imposed on the medium, with excitability decreasing with increasing light intensity.

Illumination profiles of 200×200 cells, where each cell was 0.1 mm $\times$ 0.1 mm, were projected onto the gel medium using a modified video projector, with the illumination intensity adjusted to generate an excitable medium. Waves were locally initiated by varying the light intensity ϕ according to the periodic perturbation

$$\phi = \phi_0 + \alpha \sin(2\pi\nu t), \tag{1}$$

where the pacemaker region was comprised of a 60×60 cell array in the center of the medium [26]. In order to insure that the wave initiation was resonance induced, the excitability control parameter ϕ was always maintained such that $\phi \geq \phi_{\mathrm{sn}}$, where $\phi_{\mathrm{sn}} = 8.80 \times 10^{-2}$ mW cm^{-2} corresponds to the maximum illumination possible for oscillatory behavior, above which only steady state behavior is exhibited. Because the system exhibits a subcritical Hopf bifurcation for these experimental conditions (see analysis below), the oscillatory regime extends to the global saddle-node bifurcation where the stable and unstable limit cycles coalesce. Hence, the value ϕ_{sn} corresponds to the global saddle-node bifurcation, and $\phi_{\mathrm{sn}} > \phi_H$, where ϕ_H is the light intensity corresponding to the Hopf bifurcation point. Wave initiation by changing the light intensity such that the system crosses the Hopf bifurcation point is well known in the photosensitive BZ reaction [27–29].

Figure 1 shows the resonance pacemaker in the BZ system, where panel (a) depicts the initially quiescent excitable medium, with the region of periodic perturbation in light intensity shown by the central square. As shown in panel (b), the variation of light intensity with an appropriate amplitude and frequency results in the appearance of wave activity at the center of the resonance pacemaker region. The resonance initiation forms a wave that grows and propagates outward in the form of a circular wave, as shown in panels (c)–(e). Panel (f) shows the subsequent wave being similarly initiated in the center of the pace-

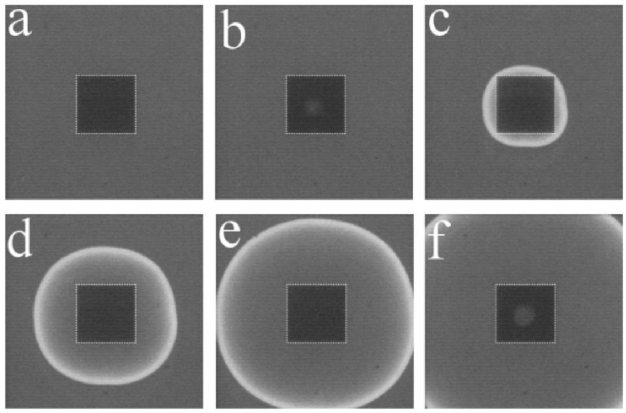

FIG. 1. Resonance initiated waves propagating into an excitable light-sensitive BZ medium. Images collected at 20.0 s intervals show the initiation of a wave in the initially quiescent medium via localized periodic modulations of light intensity according to Eq. (1), where $\phi_0 = 0.119\ \mathrm{mW\,cm^{-2}}$, $\alpha = 0.022\ \mathrm{mW\,cm^{-2}}$, and $\nu = 1.25 \times 10^{-2}\ \mathrm{s^{-1}}$. The light intensity $\phi_{\mathrm{ref}} = 0.485\ \mathrm{mW\,cm^{-2}}$ is applied to the remainder of the medium to maintain it in an excitable state. (a) The local periodic modulation in light intensity is applied to the center of the medium (dark square) in a region of 60×60 grid points ($6.0 \times 6.0\ \mathrm{mm^2}$). (b) The initiation of the wave occurs in the center of the resonance region, which then propagates outward, as shown in (c)–(e). A wave is initiated every period of the light intensity modulation, resulting in a 1:1 resonance pattern; the subsequent wave initiation is shown in (f). The reaction is carried out in an open reactor at 20.0 °C, which is supplied with fresh catalyst-free BZ solution: 0.552 M $NaBrO_3$, 0.026 M malonic acid, 0.162 M bromomalonic acid, 0.489 M H_2SO_4. Prior to mixing and equilibration to the reaction temperature, all reaction solutions were maintained at 0.0 °C to prevent decomposition. Ruthenium(II) tris-2,2′-bipyridyl, the light-sensitive catalyst, was immobilized in a silica gel medium ($0.3 \times 20 \times 20\ \mathrm{mm^3}$), prepared by acidifying a solution of 15% (w/w) $Na_2Si_3O_7$ and 1.88 mM $Ru(bpy)_3^{2+}$ with H_2SO_4. The ruthenium containing gel solution was then cast onto a microscope slide. Light from the video projector was passed through a band pass filter with a central wavelength of 460 nm, which is close to the excitation wavelength of the catalyst.

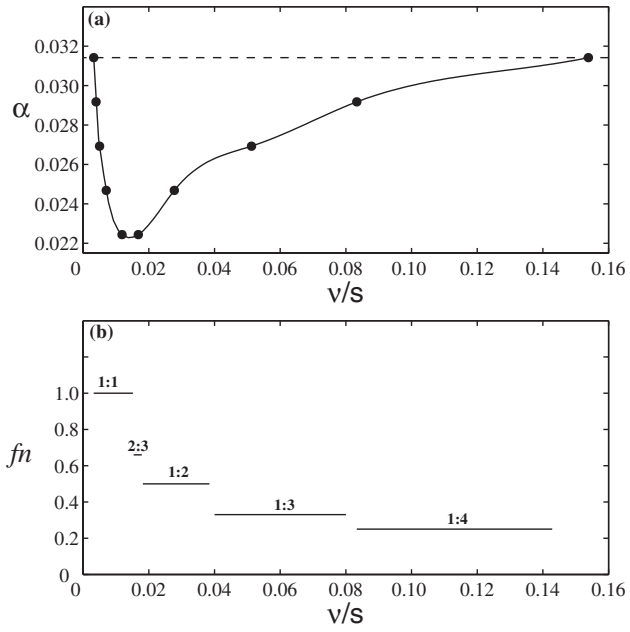

FIG. 2. (a) Domain of resonance wave initiation for forcing amplitude parameter α (in $\mathrm{mW\,cm^{-2}}$) as a function of frequency ν (in $\mathrm{s^{-1}}$). The parameter α was varied in increments of $2.2 \times 10^{-3}\ \mathrm{mW\,cm^{-2}}$ and the period was varied in increments of 1.0 s to determine the region of resonance wave initiation. The parameter value $\alpha = 0.0314\ \mathrm{mW\,cm^{-2}}$, indicated by the dotted line, corresponds to the maximum amplitude that guarantees $\phi \geq \phi_{\mathrm{sn}}$, where $\phi_{\mathrm{sn}} = 8.80 \times 10^{-2}\ \mathrm{mW\,cm^{-2}}$. Solid curve shows cubic spline fit of measured values (solid circles). The three values at highest forcing frequency ($\nu = 0.05$, 0.08, and $0.15\ \mathrm{s^{-1}}$) each represents an average of three measurements with a resolution of ± 1.0 s in period; all other values are single measurements with a 1.0 s resolution in period. (b) Firing number fn as a function of the forcing frequency for $\alpha = 0.0314\ \mathrm{mW\,cm^{-2}}$. The resonances are indicated by the number of waves initiated per number of driving cycles. Experimental concentrations and conditions are the same as in Fig. 1.

maker region. This process repeats as long as the light intensity ϕ is modulated in the pacemaker region. For the particular period and amplitude used for Fig. 1, the period of wave initiation is the same as the period of the perturbation, corresponding to a 1:1 resonance pattern. Different resonance patterns can be defined in terms of the firing number, $fn = p/q$, where p is the number of waves initiated and q is the corresponding number of driving cycles. Hence, the firing number for the wave pattern in Fig. 1 is $fn = 1$.

The forcing period and amplitude were systematically varied with the value of ϕ_0 near the oscillatory regime in order to determine the parameter region where waves can be initiated by the resonance. Figure 2(a) shows the amplitude-frequency domain for resonance pacemakers in the excitable BZ medium. We see that at and below the amplitude corresponding to the saddle-node bifurcation point ($\alpha = 0.0314\ \mathrm{mW\,cm^{-2}}$) there is a range in frequency and amplitude where waves can be initiated by resonance.

More complex resonance patterns are possible, and the firing number fn as a function of the period of the imposed sinusoidal perturbations for a fixed forcing amplitude α is shown in Fig. 2(b). Elements of a devil's staircase can be seen, with a wide region of 1:4 behavior and decreasing regions of 1:3, 1:2, and 1:1 resonances, as well as a 2:3 resonance. Because the width of the resonance region decreases with smaller forcing amplitudes, as shown in Fig. 2(a), fewer resonance patterns can be resolved at lower amplitudes.

Simulations of the resonance pacemaker were carried out using an Oregonator model [30,31] modified to account for the effects of illumination of the photosensitive Belousov-Zhabotinsky (BZ) reaction [25,32]:

$$\begin{aligned}\epsilon\partial_\tau x &= \epsilon D_x\nabla^2 x + x(1-x) + y(q-x) + p_2\phi,\\ \epsilon'\partial_\tau y &= \epsilon' D_y\nabla^2 y + 2hz - y(q+x) + p_1\phi,\\ \partial_\tau z &= D_z\nabla^2 z + x - z + \left(\frac{p_1}{2} + p_2\right)\phi,\end{aligned} \tag{2}$$

where x, y, and z represent the dimensionless concentrations of bromous acid, bromide, and the oxidized form of the catalyst, respectively, and τ is dimensionless time [33]. The parameter ϕ represents the light intensity, which serves to control the excitability of the medium. Because the Ru(III) complex is immobilized in the silica gel, the corresponding diffusion coefficient $D_z = 0$.

The dynamics of Eqs. (2) without diffusion, $D_x = D_y = D_z = 0$, was analyzed by numerical integration and linear stability analysis of the corresponding ordinary differential equations, with the light intensity ϕ serving as the bifurcation parameter [22,32]. The analysis revealed a subcritical Hopf bifurcation [32], where the global saddle-node bifurcation occurs at $\phi_{\rm sn} = 1.695 \times 10^{-3}$ and the Hopf bifurcation point occurs at $\phi_H = 1.687 \times 10^{-3}$. The system exhibits bistability between the stable steady state and the stable limit cycle for $\phi_H < \phi < \phi_{\rm sn}$ and exhibits only steady state behavior for $\phi > \phi_{\rm sn}$.

Systematically scanning the forcing period and amplitude with the value of ϕ_0 close to the oscillatory regime of Eqs. (2) reveals the region in the parameter space where waves can be initiated by resonance with the forcing. Figure 3 shows an example of a resonance pacemaker, in which the periodic forcing of the excitation occurs in the central square. A wave is formed and proceeds to propagate outward, as shown in (c) and (d). Panel (e) shows a second wave initiated by the resonance pacemaker, with the resulting wave shown in (f).

A detailed study of the resonance domain structure was carried out in simulations with a one-dimensional array, where the value of ϕ was modulated in a central pacemaker region. Figure 4(a) shows the resonance pacemaker domain, which is subdivided into regions of more complex resonances. We see regions of 1:1, 1:2, and 1:3 resonances corresponding to one wave generated for every one, two, and three forcing cycles. These subdomains are not adjacent but have gaps between them in which more complex resonance patterns are exhibited. The full complexity of the resonance patterns can be seen in Fig. 4(b), where the firing number is plotted as a function of the forcing frequency for a fixed value of α [34]. We see an almost complete devil's staircase, in which many higher-order resonances are exhibited between the gaps of the primary resonances shown in Fig. 4(a). The qualitative features of the devil's staircase are in good agreement with the experimentally determined staircase shown in Fig. 2(b). We note that the distortion of the resonance tongues gives rise to irregular devil's staircases at lower values of α, for ex-

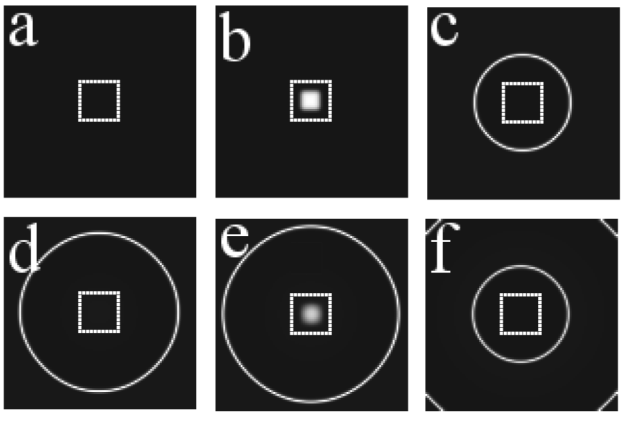

FIG. 3. Resonance pacemaker simulated with Eqs. (2) in a two-dimensional domain of 100×100 grid points ($\Delta x = 0.02$, $\Delta t = 0.0001$). The resonance region is 20×20 grid points in the center of the domain (dotted square), in which the illumination intensity is modulated according to Eq. (1). Images show behavior at $\tau = 90$ (a), 100 (b), 150 (c), 190 (d), 201 (e), and 250 (f). Control parameters: $\alpha = 3.24 \times 10^{-4}$ and $\nu = 0.01$.

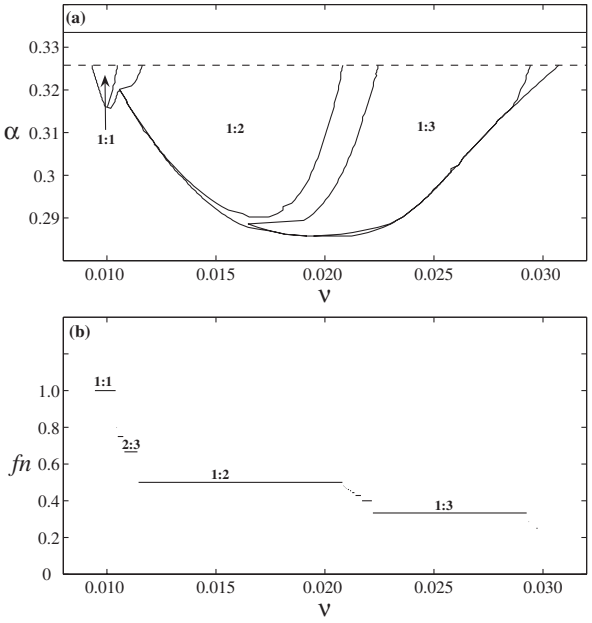

FIG. 4. (a) Domain of resonance wave initiation for amplitude parameter α as a function of frequency ν, computed from Eqs. (2). The α values are scaled by a factor of 10^3. Shown within the resonance pacemaker domain are mode-locking regions with 1:1, 1:2, and 1:3 resonances, with higher resonances occurring between these regions. The simulation was carried out using a one-dimensional array of 50 grid points ($\delta x = 0.02$, $\delta t = 0.0001$). The parameter ϕ (light intensity) was maintained at 2.021×10^{-3} everywhere except in a pacemaker region of 20 grid points, where it was modulated according to Eq. (1) with $\phi_0 = 2.021 \times 10^{-3}$. The dashed line at $\alpha = 0.326 \times 10^{-3}$ shows the value of the amplitude parameter necessary to reach the saddle-node bifurcation point at $\phi_{\rm sn} = 1.695 \times 10^{-3}$. The solid line at $\alpha = 0.333 \times 10^{-3}$ shows the value of the amplitude parameter necessary to reach the Hopf bifurcation point at $\phi_H = 1.687 \times 10^{-3}$. (b) Firing number fn as a function of the forcing frequency for $\alpha = 0.324 \times 10^{-3}$. The resonances are indicated by the number of waves initiated per number of driving cycles.

ample, where the gap between the 1:2 and 1:3 resonances curls below the 1:2 resonance. Higher resolution simulations show that the 1:3 resonance tongue along with the higher resonances curl below and to the left of the 1:2 resonance. Distorted resonance tongues have also been observed in the resonant phase patterns of a periodically forced BZ system [35,36].

Our experiments and simulations show that small, local modulations of excitability give rise to wave initiations in a quiescent excitable medium, where the medium is globally transformed from a stationary state to an oscillatory state of successive traveling waves. The resonance pacemaker may have practical implications in biological systems, since resonances between physiological oscillators commonly occur. Such wave sources in cardiac tissue could have pathological consequences [19,37]. The resonance pacemaker represents a new mechanism for wave formation in excitable media.

We thank the National Science Foundation (CHE-0415392) and the W. M. Keck Foundation for supporting this research. We also thank Mark Tinsley and Aaron Steele for technical assistance and valuable discussions.

[1] A. N. Zaikin and A. M. Zhabotinsky, Nature (London) **225**, 535 (1970).
[2] A. T. Winfree, Sci. Am. **230**, 82 (1974).
[3] A. T. Winfree, *The Geometry of Biological Time* (Springer, New York, 1980).
[4] A. Pagola and C. Vidal, J. Phys. Chem. **91**, 501 (1987).
[5] E. Mori and J. Ross, J. Phys. Chem. **96**, 8053 (1992).
[6] K. Suzuki, T. Yoshinobu, and H. Iwasaki, Chem. Phys. Lett. **349**, 437 (2001).
[7] K. Showalter and R. M. Noyes, J. Am. Chem. Soc. **98**, 3730 (1976).
[8] K. Showalter, R. M. Noyes, and H. Turner, J. Am. Chem. Soc. **101**, 7463 (1979).
[9] R. J. Field, E. Körös, and R. M. Noyes, J. Am. Chem. Soc. **94**, 8649 (1972).
[10] A. T. Winfree, Science **175**, 634 (1972).
[11] J. D. Murray, *Mathematical Biology* (Springer, New York, 1989).
[12] S. Grill, V. S. Zykov, and S. C. Müller, J. Phys. Chem. **100**, 19 082 (1996).
[13] A. T. Winfree, J. Theor. Biol. **138**, 353 (1989).
[14] N. Shibata, P. Chen, E. G. Dixon, P. D. Wolf, N. D. Danieley, W. M. Smith, and R. E. Idekar, Am. J. Physiol. **255**, H891 (1988).
[15] J. M. Davidenko, P. Kent, and J. Jalife, Physica D (Amsterdam) **49**, 182 (1991).
[16] J. Maselko and K. Showalter, Physica D (Amsterdam) **49**, 21 (1991).
[17] O. Steinbock, P. Kettunen, and K. Showalter, Science **269**, 1857 (1995).
[18] I. R. Epstein and V. K. Vanag, Chaos **15**, 047510 (2005).
[19] J. M. Davidenko, A. M. Pertsov, R. Salomonsz, W. Baxter, and J. Jalife, Nature (London) **355**, 349 (1992).
[20] A. T. Winfree in *Oscillations and Traveling Waves in Chemical Systems*, edited by R. J. Field and M. Burger (Wiley, New York, 1985), p. 441.
[21] M. Gómez-Gesteira, G. Fernandez-Garcia, A. P. Muñuzuri, V. Pérez-Muñuzuri, V. I. Krinsky, C. F. Starmer, and V. Pérez-Villar, Physica D (Amsterdam) **76**, 359 (1994).
[22] P. Parmananda, H. Mahara, T. Amemiya, and T. Yamaguchi, Phys. Rev. Lett. **87**, 238302 (2001).
[23] L. Kuhnert, Nature (London) **319**, 393 (1986).
[24] H. J. Krug, L. Pohlmann, and L. Kuhnert, J. Phys. Chem. **94**, 4862 (1990).
[25] S. Kádár, T. Amemiya, and K. Showalter, J. Phys. Chem. A **101**, 8200 (1997).
[26] The size of the pacemaker region in the experiments and simulations was set larger than the critical size for resonance initiated waves in order to obtain the best reproducibility. The critical size was found to be approximately 1.5×1.5 mm^2 for the experimental system and approximately 11×11 grid points in the simulations.
[27] J. Wang, S. Kádár, P. Jung, and K. Showalter, Phys. Rev. Lett. **82**, 855 (1999).
[28] S. Alonso, I. Sendiña-Nadal, V. Pérez-Muñuzuri, J. M. Sancho, and F. Sagués, Phys. Rev. Lett. **87**, 078302 (2001).
[29] M. Tinsley, J. Cui, F. V. Chirila, A. Taylor, S. Zhong, and K. Showalter, Phys. Rev. Lett. **95**, 038306 (2005).
[30] R. J. Field and R. M. Noyes, J. Chem. Phys. **60**, 1877 (1974).
[31] J. J. Tyson and P. C. Fife, J. Chem. Phys. **94**, 4862 (1990).
[32] T. Amemiya, T. Ohmori, M. Nakaiwa, and T. Yamaguchi, J. Phys. Chem. A **102**, 4537 (1998).
[33] The dimensionless quantities and their dimensional counterparts are related by the following [25,32]: $x = \frac{2k_{O4}}{k_{O3}A} X$, $y = \frac{k_{O2}}{k_{O3}A} Y$, $z = \frac{k_{O4}k_{O5}M}{(k_{O3}A)^2} Z$, $\tau = k_{O5}Mt$. The dimensionless parameters are defined according to $\epsilon = \frac{k_{O5}M}{k_{O3}A}$, $\epsilon' = \frac{2k_{O4}k_{O5}M}{k_{O2}k_{O3}A}$, $q = \frac{2k_{O1}k_{O4}}{k_{O2}k_{O3}}$, $\phi = \frac{2k_{O4}}{(k_{O3}A)^2}\Phi$, $p_1 = \frac{V}{0.089+V+2.05A}$, $p_2 = \frac{2.05A}{0.089+V+2.05A}$, and the parameters are $k_{O1} = (2\ \mathrm{M}^{-3}\,\mathrm{s}^{-1})\mathrm{H}^2$, $k_{O2} = (3 \times 10^6\ \mathrm{M}^{-2}\,\mathrm{s}^{-1})\mathrm{H}$, $k_{O3} = (42\,\mathrm{M}^{-2}\,\mathrm{s}^{-1})\mathrm{H}$, $k_{O4} = 3 \times 10^3\,\mathrm{M}^{-1}\,\mathrm{s}^{-1}$, $k_{O5} = 5\ \mathrm{M}^{-1}\,\mathrm{s}^{-1}$, $h = 0.5$, $H = 0.37$ M, $A = 0.15$ M, $M = 0.2$ M, $V = 0.05$ M. The diffusion constants are $D_x = 1.5 \times 10^{-5}$, $D_y = 1.68 \times 10^{-5}$, and $D_z = 0$. The parameter Φ represents the rate of photochemical production of bromide ion (Y) and is proportional to the light intensity [25].
[34] Waves are initiated at all frequencies for amplitudes approaching the Hopf bifurcation point, $\alpha = 0.333 \times 10^{-3}$, above the saddle-node bifurcation point, $\alpha = 0.326 \times 10^{-3}$ (see Fig. 4). However, waves are not initiated outside the resonance envelope for amplitudes at and above the saddle-node bifurcation point. Specifically, no waves were initiated at $\nu = 0.009$ and 0.031 for $\alpha = (0.326, 0.327, 0.328, 0.329) \times 10^{-3}$.
[35] A. L. Lin, M. Bertram, K. Martinez, A. Ardelea, G. F. Carey, and H. L. Swinney, Phys. Rev. Lett. **84**, 4240 (2000).
[36] A. L. Lin, A. Hagberg, E. Meron, and H. L. Swinney, Phys. Rev. E **69**, 066217 (2004).
[37] Y. Nagai, H. Gonzales, A. Shriver, and L. Glass, Phys. Rev. Lett. **84**, 4248 (2000).